

# Numerical Study of Heat Transfer Enhancement in A Solar Tower Power Receiver, Through the Introduction of Internal Fins

Open  
Access

Hashem Shatnawi<sup>1,3,\*</sup>, Chin Wai Lim<sup>1</sup>, Firas Basim Ismail<sup>2</sup>, Abdulrahman Aldossary<sup>3</sup>

<sup>1</sup> Mechanical Engineering Department, College of Engineering, Universiti Tenaga Nasional, 43000 Kajang, Selangor, Malaysia

<sup>2</sup> Power Generation Unit, Institute of Power Engineering (IPE), Universiti Tenaga Nasional, 43000 Kajang, Selangor, Malaysia

<sup>3</sup> Jubail Technical Institute, PO Box 10335, Jubail Industrial City 31961, Saudi Arabia

## ARTICLE INFO

## ABSTRACT

### Article history:

Received 3 April 2020

Received in revised form 22 May 2020

Accepted 24 May 2020

Available online 15 August 2020

In the context of solar tower power, the significance of the receiver has to do with its capacity to convert sun rays into heat. This heat is then conveyed to a heat transfer fluid. The extremely high velocity of the heat transfer fluid, motivates for the use of smart geometry to simultaneously enhance the heat transfer process and strengthen the structure of the tubes. In this study, a new molten salt receiver design was numerically investigated, following the addition of square, rectangular, circular and triangular longitudinal fins, that come at various heights ( $w=1,2,4$  and  $6$  mm). Molten salt was used as the heat transfer fluid that flown through the receiver tubes with the Reynolds number ranging between 14,000 and 38,000. In comparison to a smooth tube, it was observed that while the inclusion of fins led to a dip in pressure, the overall efficiency level was improved. An increase in the number of fins, led to an improvement in the heat transfer process. The use of four square fins delivered the highest heat transfer enhancement. In the use of a singular fin, a triangular fin with a height of 1 mm delivered the best heat transfer performance. For a similar flow rate and hydraulic area, the triangular fins exhibited a better heat transfer performance than the square, circular and rectangular fins. In terms of the receiver's efficiency, the triangular fins produced the heights efficiency.

### Keywords:

Solar Tower; External Receiver; Internal Fins; Turbulent Flow; Nusselt Number; Mathematical Model

Copyright © 2020 PENERBIT AKADEMIA BARU - All rights reserved

## 1. Introduction

Solar tower power systems belong to an area of technology that focuses on the exploitation of heat energy from the sun. The reflection of concentrated solar radiation onto a fluid medium, serves to produce heat, which is harnessed for the generation of electricity. In solar tower power systems,

\* Corresponding author.

E-mail address: [hashem121@yahoo.com](mailto:hashem121@yahoo.com)

<https://doi.org/10.37934/arfmts.74.1.98118>

a large number of flat, sun-tracking mirrors, known as heliostats, direct sunlight onto a receiver at the top of a tall tower. This is illustrated in Figure 1.

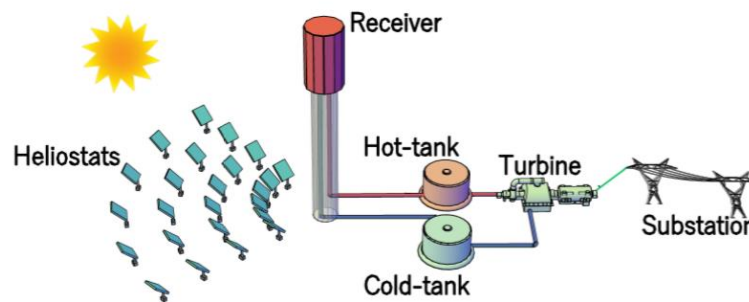


Fig. 1. Solar power tower plant

Solar energy has drawn the attention in a wide variety of fields, as energy derived from sun rays is not only inexhaustible, but also environmentally friendly [1]. During the last decade, the emphasis on central receiver systems (CRS) can be attributed to the drastic increase in the price of fossil fuels, and the detrimental environmental effects associated to their burning. Among several choices available, solar power tower energy is highly favoured, for meeting the constantly growing demand for energy [2].

The receiver used in commercial solar tower power plants, is known as an external tube receiver. The external receiver is considered a major component of the solar power tower. While half the circumference of the tube is heated by solar rays reflected from heliostats, the other half is deemed adiabatic. The efficiency and durability of a solar plant, is highly dependent on the performance of the receiver. Taking into consideration the extreme working conditions involved in solar energy generation by using the external receiver. It receives high incident solar flux on the external face, while dealing with a corrosive internal environment. Thus, the resilience of the receiver is among the most important considerations, during the development of a solar power tower. The efficiency of the receiver significantly determines the performance of the plant, and the energy cost involved.

There have been a number of works done to enhance the external receiver's performance. However, no studies have examined the effect of internally addition of fins along the external receiver to the thermal performance of the receiver. This study aims to design a new high-temperature molten salt receiver that can perform better than the conventional receiver, lessen thermal losses by utilising small diameter tubes accompanied with internal fins to minimise the external area exposed to solar rays.

Fins inside a tube serve to increase the area of heat transfer in the tube, which consequently enhances convective heat transfer. Nandakumar *et al.*, [3] studied laminar flow inside a triangular finned tube using the finite element method. He observed that the flow velocity in a finned tube is less than in a smooth tube. This is attributed to the larger wetted surface area in the finned tube. In an investigation on heat transfer in a solar receiver, Amina *et al.*, [4] observed that the use of longitudinal triangular and rectangular fins in parabolic trough solar Receiver, with nano fluid and non-uniform heat flux, affected the outer surface of the tube. A significant improvement in heat transfer is derived, when the Reynolds number is greater than 25,700. In an investigation conducted by Piña-Ortiz *et al.*, [5], it was revealed that a solar tower receiver fitted with cylindrical internal fins, increases the contact area by 225%.

The receiver's maximum thermal efficiency decreases with the incident radiative flux, and increases with the mass flow. Yang *et al.*, [6] studied the effect of non-uniform heat flux on the

external receiver of a solar tower, with molten salt as the heat transfer fluid in a bare tube. The length of the tube was 1m, the external diameter was 20mm and the internal diameter was 16mm. This study revealed that the heat flux increased with the increase in velocity. Hussein *et al.*, [7] experimentally investigated the influence of finned tubes on the performance of solar water heaters. He reported that the attendance of fins improved the temperature homogeneity in the molten wax.

Following a numerical investigation, Muñoz *et al.*, [8] revealed that the use of internal helical fin tubes, in a parabolic trough tube, raises the level of efficiency by 3%. There was an observed increase in pressure losses as the amount of fins increased. However, there was a reduction in the thermal losses and the temperature gradient. Ravi *et al.*, [9] utilised a porous disc receiver to improve heat transfer characteristics. However, a pressure drop was observed. Gong *et al.*, [10] increased the overall heat transfer performance by inserting a pin fin arrays in a parabolic trough receiver. It was observed that the average Nusselt number rose up to 9.0%.

Table 1 provides a summary of several investigations conducted on the external receiver.

**Table 1**  
Summary of literature review

Author	Year	Focus of work	Work objectives	Solution method	Outcomes
Rodríguez <i>et al.</i> , [11]	2014	Central-Tube	New design of central receiver involving several vertical panels formed by bayonet tubes, and joined on one side by a bayonet end-cap	Numerical	The use of bayonet receivers caused the salt outlet temperature to surpass 50C
Zheng <i>et al.</i> , [12]	2017	Central-Tube	Thermal analysis of solar central receiver tube with porous inserts and non-uniform heat flux	Numerical	A porous medium enhances the heat transfer performance
Chang <i>et al.</i> , [13]	2015	Tube with twisted tapes.	Study the various parameters of twisted tapes	Numerical	The insertion of twisted tape can significantly improve the temperature distribution uniformity of the tube wall and molten salt
Garbrecht <i>et al.</i> , [14]	2013	Hexagonal-pyramid shaped	CFD-simulation of a new receiver design for a molten salt solar power tower	Numerical	Most of the radiative losses are re-absorbed by the neighbouring pyramids
Zhang <i>et al.</i> , [15]	1996	Thermal energy storage system in solar energy utilization systems	Heat transfer enhancement by way of an internally finned tube	Solved by a finite difference method	The introduction of internal fins efficiently enhances the transference of heat
Liu <i>et al.</i> , [16]	2018	Four types of inserts in receiver: twisted-tape, outer finned, inclined ribs tube, and helical-line	Increase the outlet temperatures in a cavity receiver tube of a solar power tower plant	Numerical	The twisted-tape provide better performances than other three inserts

As frequently stated in relevant literature, the cosine angle of radiation (as illustrated in Figure 2) affects both the heat flux concentration, and the heat transfer performance. The receiver's homogeneous wall temperature reduces thermal stresses and the likelihood of premature receiver failure. A higher allowable heat flux leads to an improved receiver performance. Various measures have been taken to improve the maximum allowable heat flux. These measures include the use of a better material for the development of the tube and the addition of internal fins.

Finned tube is commonly used to improve convective heat transfer [17-18]. The receiver thermal efficiency improves with a decrease in the diameter of the tube. This is attributed to the reduction in heat loss [19]. The objective at all times is the maximization of flux, while reducing the receiver area. The increase in receiver thickness will lead to a decrease of pressure stresses and inner surface temperature. Hence, the level of thermal stress will be elevated [20]. This situation can be avoided through the addition of internal fins.

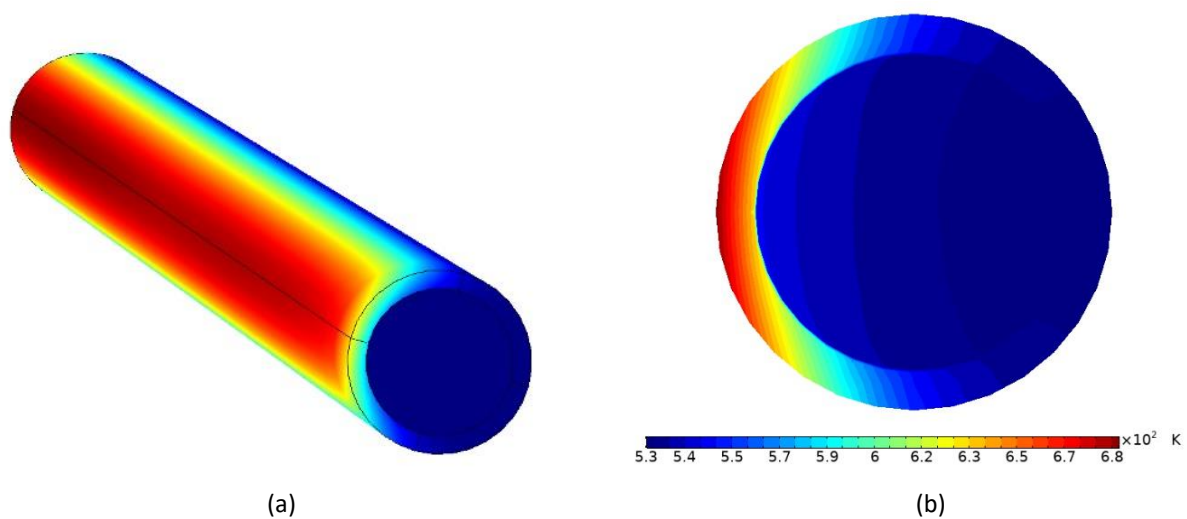


**Fig. 2.** The effect of the cosine angle on heat flux distribution along the tube a) full length, b) cross section

## 2. Mathematical Model

According to Cengel and Ghajar [21] Mathematical modelling of physical problems can be summarized in Figure 3.

### 2.1 Physical Model

Figure 4 portrays the physical model of a single tube with a length of 1.3 m, an outer-diameter ( $D_{out}$ ) of 20 mm, and an inner-diameter ( $D_{in}$ ) of 16 mm. Half of the tube (the heating surface) faces the heat flux while the other half is considered an adiabatic surface. The heat flux distribution along the cylindrical tube reflected from a surrounding field of heliostats [22] can be calculated through the equation  $q_{net} = q_{max} \cdot \cos\theta$ , where  $q_{max}$  is the maximum heat flux. The heat transfer fluid (molten salt) is passed through the inlet of the tube, which has an initial temperature of  $T_{in} = 523$  K. Subsequent to the absorption of heat, the heat transfer fluid exits the tube's outlet with an increased temperature  $T_{out}$ .

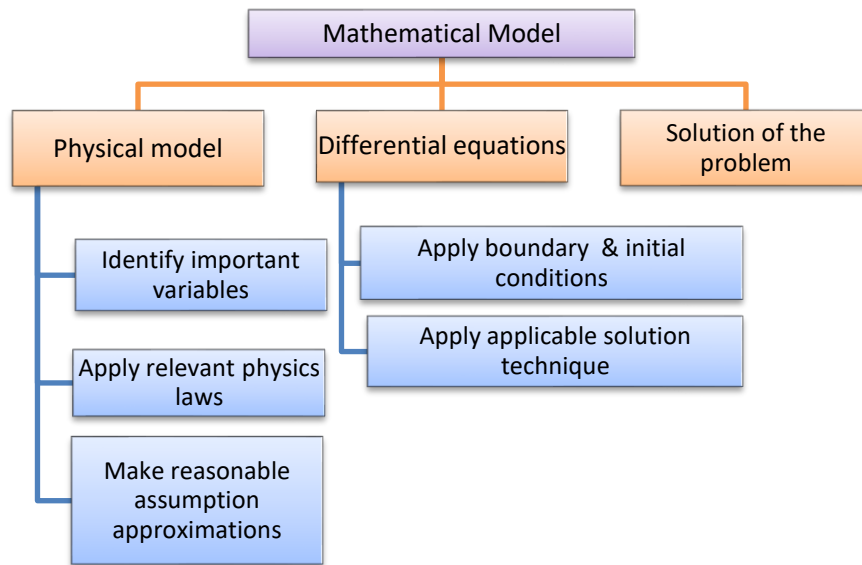


**Fig. 3.** Mathematical modeling of physical problems

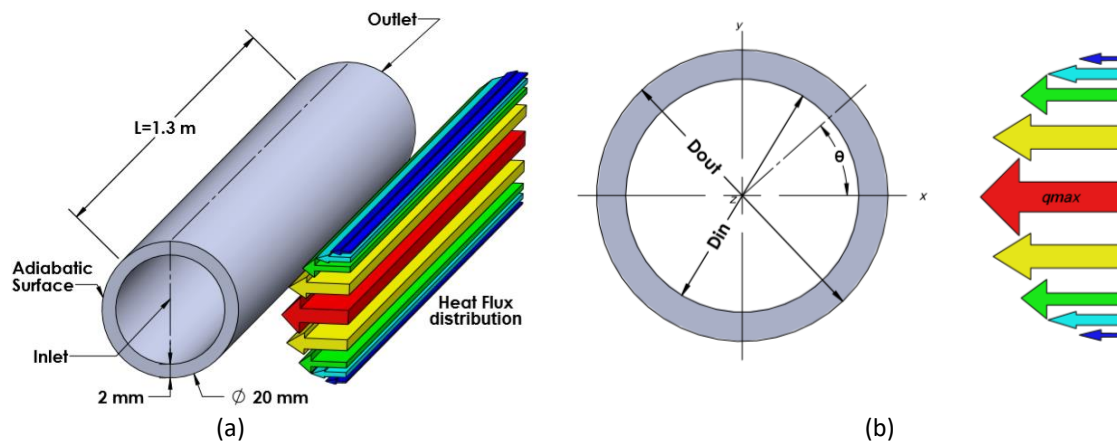


**Fig. 4.** (a) Single tube parameters with heat flux distribution, (b) Cross section of the tube

## 2.2 Fins Configurations

Four types of fins (square, rectangular, circular and triangular) were added along the tube's internal wall, as shown in Figure 5(a). Figure 5(b) provides a schematic diagram of the locations and dimensions of the fins, where  $e$  is the thickness of the fins,  $w$  is the height of the fins,  $n$  is the number of fins and  $l$  is the length along the tube. Table 2 displays the dimensions of the fins.

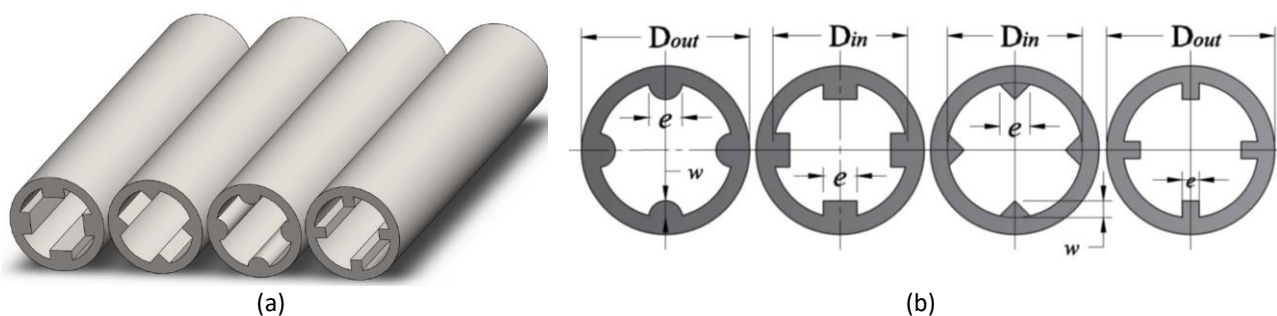


**Fig. 5.** (a) 3D shape of fins added to the tube, (b) Schematic diagram of the locations and dimensions of the fins

**Table 2**  
 Fins dimensions

Fins shape	$e$ [mm]	$w$ [mm]	$l$ [m]
Square	2	2	1.3
Rectangle	4	2	1.3
Triangle	4	2	1.3
Round	4	2	1.3

### 2.3 Molten Salt and Tube Properties

Alloy of Nickel–Chromium ( alloy 625) is selected as the receiver tube material, the density ( $\rho_s$ ) equal to  $8440 \text{ kg/m}^3$ , the thermal conductivity ( $k_s$ ) equal to  $16.3 \text{ W/m.K}$ , and specific heat ( $C_p$ )<sub>s</sub> is  $505 \text{ J/kg.K}$ , this alloy was selected because of it is high strength, corrosion resistance and exceptional fabricability [6]. The heat transfer fluid for the current study is the nitrate salt which is a mixture of sodium nitrate by 60% weight ( $\text{NaNO}_3$ ) and potassium nitrate by 40% weight ( $\text{KNO}_3$ ). It has a low vapor pressure and chemically stable. The density, specific heat, and viscosity of the molten salt can be found in Zavoico [23].

### 2.4 Physics Law

The rate of convection heat transfer in the test tube  $Q$  can be calculated from equation

$$Q = h A(T_w - T_b) \quad (1)$$

where,  $T_w$  is wall surface temperatures along the tube [K],  $T_b$  is the bulk temperature[K],  $h$  is heat transfer coefficient [ $\text{W/m}^2.\text{K}$ ], and  $A$  is a cross section area [ $\text{m}^2$ ].  $T_b$  can be found by using Eq. (2)

$$T_b = (T_{in} + T_{out})/2 \quad (2)$$

Heat transfer rate can be calculated also from Eq. (3)

$$Q = m_f c_p(T_{out} - T_{in}). \quad (3)$$

Heat transfer coefficient can be obtained from

$$h = \frac{q}{(T_w - T_b)} = \frac{m_f c_p(T_{out} - T_{in})}{A(T_w - T_b)} \quad (4)$$

Here,  $q$  and  $m_f$  are the heat flux of the pipe in  $\text{W/m}^2$  and mass flow rate of the molten salt in  $\text{kg/sec}$ , respectively.  $C_p$  is the specific heat capacity of molten salt in  $\text{J/kg K}$ .

For cylindrical tube, conduction heat transfer rate is:

$$\dot{Q} = -2\pi L k_s \frac{(T_w - T_\infty)}{\ln(D_{out}/D_{in})} \quad (5)$$

where  $\dot{Q}$  the conduction heat transfer rate in  $\text{W}$ ; and  $T_\infty$  is the outer surface temperature[K], and  $L$  is the receiver length [m].

$$T_w = T_\infty - \frac{\dot{Q}}{2\pi L k_s} \ln\left(\frac{D_{out}}{D_{in}}\right) \quad (6)$$

The mean temperature of a fluid flowing through a circular pipe at length  $x$  is expressed as

$$T_b(x) = T_{b_i} + \frac{q\pi D_h}{m_f c_p} x \quad (7)$$

Average Nusselt number is defined as

$$Nu = \frac{D_h}{k} \cdot \frac{\bar{q}}{(\bar{T}_w - \bar{T}_b)} \quad (8)$$

$$D_h = \frac{4A}{P} \quad (9)$$

where

$D_h$ : hydraulic diameter [m];  $A$ : cross section area [m<sup>2</sup>];  $P$ : perimeter [m];  $k$ : molten Salt thermal conductivity [W/m.K];  $\bar{q}$ : average Heat flux [W/m<sup>2</sup>];  $\bar{T}_w$ : average wall temperature of inner wall;  $\bar{T}_b$ : average bulk temperature.

Reynolds number can be defined as

$$Re = \frac{\rho u_{in} D_h}{\mu} \quad (10)$$

where,  $\rho$ : molten salt density [Kg/m<sup>3</sup>],  $\mu$ : salt viscosity [kg/m s],  $u_{in}$ : inlet velocity [m/sec].

### 2.5 Heat Transfer Classical Correlations in a Tube

Dittus-Boelter correlation which is valid for Reynolds number greater than 10,000 Prandtl number ( $Pr$ ) between 0.7 to 120, and the ratio between length to diameter greater than 60 [24-25].

$$Nu = 0.023 Re^{0.8} Pr^{0.3} \quad (11)$$

The overall thermal performance is presented in terms of the Thermal Enhancement Factor ( $TEF$ ) [26].

$$TEF = \left(\frac{Nu}{Nu_o}\right) \left(\frac{f}{f_o}\right)^{-1/3} \quad (12)$$

where  $Nu_o$  is the Average Nusselt number for smooth tube (circular tube),  $f_o$  is the Darcy friction factor for smooth tube (circular tube).

Fraction factor is defined as:

$$f = \frac{\Delta p}{\left(\frac{1}{2}\rho u^2\right)(L/D_h)} \quad (13)$$

where  $\Delta p$  is the pressure drop [Pa] and  $u$  is average velocity [m/sec].

The receiver performance parameter ( $\eta$ ) of the modified external receiver is obtained from Eq. (14).

$$\eta = \frac{Q}{q_{max} \cdot A_E} = \frac{m_f c_p (T_{out} - T_{in})}{q_{max} \cdot A_E} \quad (14)$$

where  $A_E$  is the external receiver area [ $m^2$ ] and  $q_{max}$  is the maximum applied heat flux [ $W/m^2$ ].

## 2.6 Governing Equations

The Governing Equations for Incompressible flow, newtonian and steady state flow with constant fluid properties can be written as [27]:

Mass conservation equation:

$$\frac{\partial(\rho u_i)}{\partial x_i} = 0 \quad (15)$$

Momentum equation:

$$\frac{\partial(\rho u_i u_j)}{\partial x_i} = -\frac{\partial p}{\partial x_i} + \frac{\partial y}{\partial x_j} \left[ (\mu_t + \mu) \left( \frac{\partial u_i}{\partial x_j} + \frac{\partial u_j}{\partial x_i} - \frac{2}{3} \frac{\partial u_l}{\partial x_l} \delta_{ij} \right) \right] + \rho g_i \quad (16)$$

Energy equation:

$$\frac{\partial(\rho u_i h)}{\partial x_i} = \frac{\partial}{\partial x_i} \left[ c_p \left( \frac{\mu}{Pr} + \frac{\mu_t}{Pr_t} \right) \frac{\partial T}{\partial x_i} \right] \quad (17)$$

where

$u_i$ : component of velocity [ $m \cdot s^{-1}$ ];  $\mu$ : dynamic viscosity of fluid [ $Pa \cdot s$ ];  $\mu_t$ : turbulent viscosity of flow [ $kg \cdot m^{-1} \cdot s^{-1}$ ];  $Pr$ : nondimensional Prandtl number;  $\delta_{ij}$ : unit tensor;  $Pr_t$ : turbulent Prandtl number of energy;  $g$ : gravity [ $m \cdot s^{-2}$ ];  $h$ : specific enthalpy [ $J \cdot kg^{-1}$ ], convective heat transfer coefficient [ $W \cdot m^{-2} \cdot K^{-1}$ ].

## 2.7 Boundary Conditions

The boundary conditions which used to solve the system of nonlinear partial differential equation conditions can be summarized in Table 3.

The  $k$ -epsilon model is the most commonly used engineering turbulence model among industrial applications. This robust model is considered fairly accurate. In other words, it offers a more exact description of how turbulence affects the mean flow and is able to more accurately capture the effects of near-wall turbulence. Two equations are presented in the model; the first equation is for the turbulent kinetic energy, while the second equation is for the rate of turbulent dissipation[28].

**Table 3**  
 Domain Boundary conditions

Boundary location	Boundary condition
Inlet	$u=u_{in}$ (Different value based on Re and $D_h$ ) $v=w=0$ $T=T_{in}=523$ [K] $p=p_i=1$ [atm]
Fully developed condition	$\frac{\partial u}{\partial x} = \frac{\partial v}{\partial x} = \frac{\partial w}{\partial x} = 0$
Symmetrical flow	Fluid Domain: $\frac{\partial u}{\partial y} = \frac{\partial v}{\partial y} = \frac{\partial w}{\partial y} = \frac{\partial p}{\partial y} = 0$ Solid domain $u=v=w=0$
Adiabatic walls	$u = v = w = 0$ $\frac{\partial T}{\partial x} = 0$
The inner surface of receiver (no-slip)	$T_f = T_w$
Heat Flux	$q_{net} = q_{max} \cos\theta; -90^\circ \leq \theta \leq 90^\circ$
Half of the tube	$q_{max} = 400 \text{ kW/m}^2$

### 3. Grid Independency

COMSOL Multiphysics 5.5 was utilised to obtain the solution of the governing equations of heat transfer and fluid flow. Importation of the tube took place from SolidWorks to COMSOL. The types of solid and fluid were specified from the material library, before selecting the governing equations for examining the pressure drop and the heat transfer. Boundary conditions were then implemented within the domain.

In order to define the lowest number of grid cells to guarantee that the present numerical simulation is independent of the grid cells, COMSOL offers several ways of generating the mesh for domain after selecting predefined physics controlled meshes that are titled as extremely-coarse, extra-coarse, coarser, coarse, normal, fine, finer, extra-fine, and extremely-fine. By choosing one of these options, the program constructs the mesh automatically with predefined mesh size parameters. Figure 6(a) demonstrates the relative error for the average temperature of the outlet against the grid density at  $Re=14,000$ . The relative error's decreasing profiles can obtain very minute values, reaching a  $1.5E-04$  value for the finer mesh with the amount of elements equalling to  $N = 920,000$ . This was selected as ideal as any larger quantities of elements which did not generate a significant transformation of resulting temperatures. Figure 6(b) shows the meshing applied to computational domain.

#### 3.1 Validation

For the same tube dimensions, tube material, heat transfer fluid, and the boundary conditions; a comparison between the Nusselt number calculated by COMSOL 5.5, and the numerical and experimental values in Yang [6], as well as the Dittus-Boelter correlation, revealed good agreement with the numerical Nu numbers in trend. As explained by Yang [6], a deviation within the experimental values is  $\pm 7.5\%$ , over a Reynolds number (Re) range. This deviation is attributed to the fact that the properties of the molten salt used for the experiment, differ slightly from the properties of molten salt used for simulation. While the heat flux received by the receiver is not constant, the discrepancy between the Dittus-Boelter correlation and the obtained result increases in tandem with

the increase in Re [29]. The deviation of roughly 9% derives from correlation which is based on experimental data, and a uniform heat flux. The validation test of a smooth tube, with Reynolds numbers ranging between 14000 and 38000, with molten salt fluid, is portrayed in Figure 7.

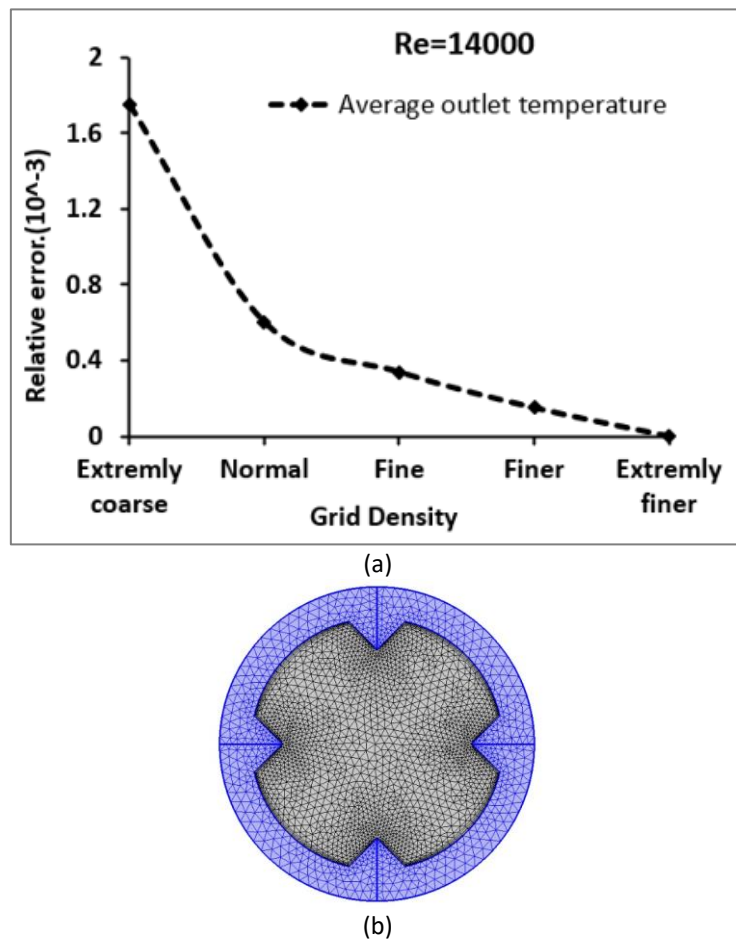


**Fig. 6.** (a) Relative error versus the grid density, (b) Cross section of mesh domain

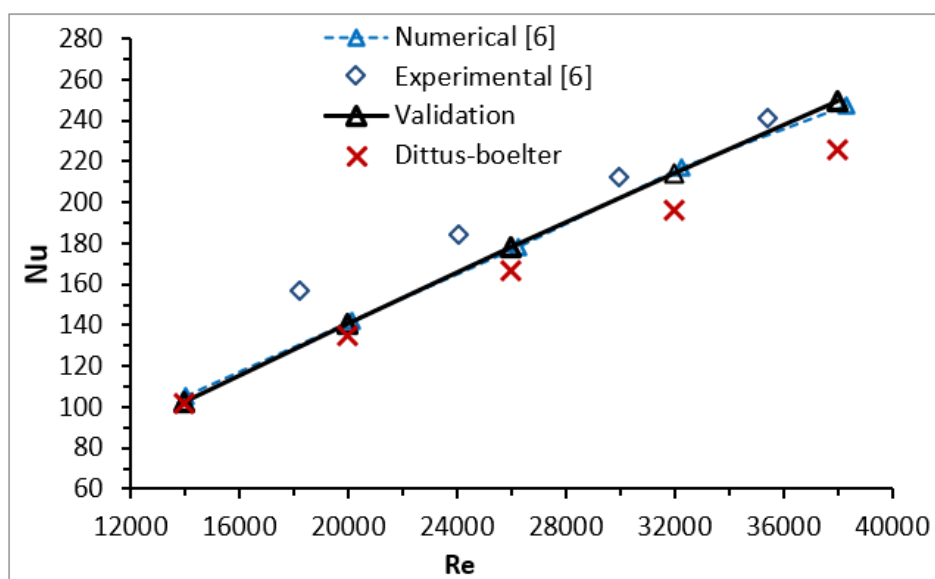


**Fig. 7.** Comparison of average Nusselt numbers with regards to a circular smooth tube

## 4. Results

Turbulent forced convection flow was investigated numerically over Reynolds numbers ranging between 14,000 and 38,000. A molten salt receiver with fins of different shapes was proposed, to improve thermal behaviour under operating conditions.

### 4.1 Internal Square, Triangular, Circular and Rectangular Finned Tubes

The average Nusselt number calculated with  $w=2$  and  $n=1, 3$  and  $4$ , revealed the  $Nu$  to be directly proportional to the  $Re$  number. It is clear that an increase, in the velocity of the fluid, increases the turbulence in the flow. This gave rise to an enhancement in convection, as well as a climb in the average Nusselt number.

Figure 8 illustrates the effect arising from the addition of internal fins to the receiver tube. It is obvious that the  $Nu$  value grew in tandem with the increase in  $n$ , and that a decrease in the number of fins reduced the  $Nu$  value. Furthermore, the addition of internal fins led to different flow patterns. The increase in turbulence, arising from this situation, interrupts the development of the boundary layer, to render the molten salt boundary layer thin. The resulting increase in flow rate and turbulence intensity served to enhance the heat transfer performance. The addition of fins also led to a reduction in the hydraulic diameter, which considerably increased the flow velocity. This culminated in an enhancement in convection, as well as an improvement in heat transfer. For  $n=4$ , and when the Reynolds number increased from 14,000 to 38,000, the  $Nu$  in the square fins tube rose from 114.53 to 258.8. In the use of triangular fins with  $n=4$ , the value of  $Nu$  with  $Re=14,000$  was recorded as 111.1. However, when  $Re=38,000$ , the  $Nu$  increased to 260.45.

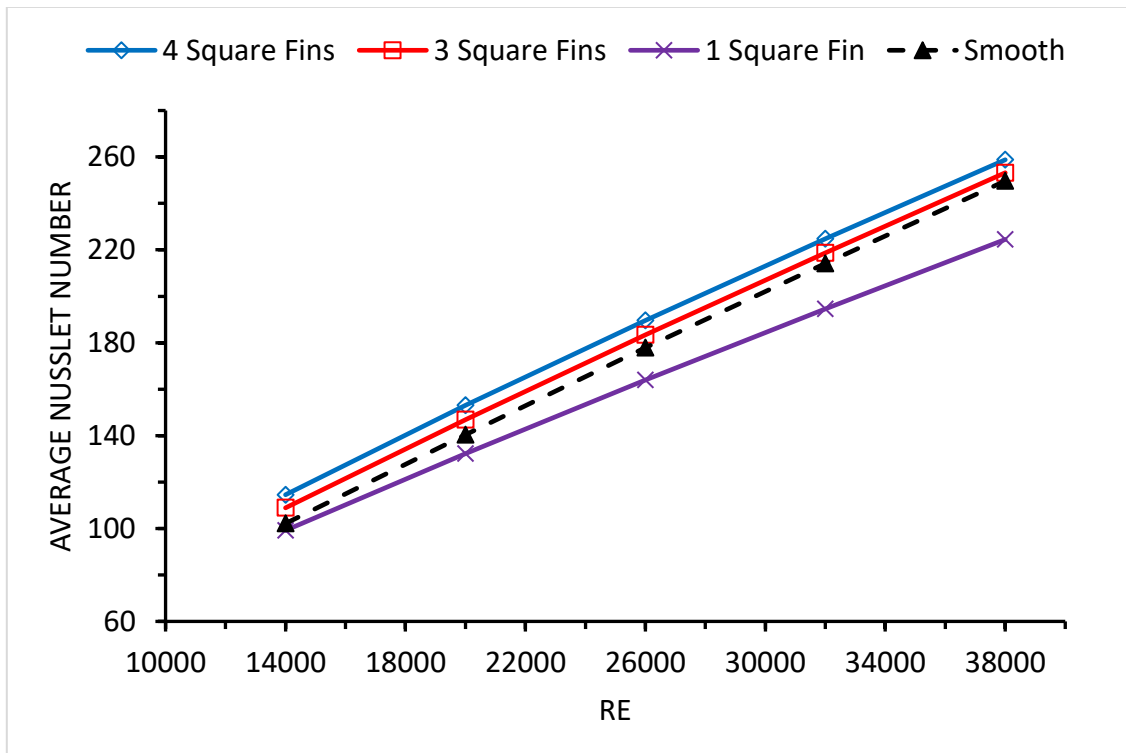
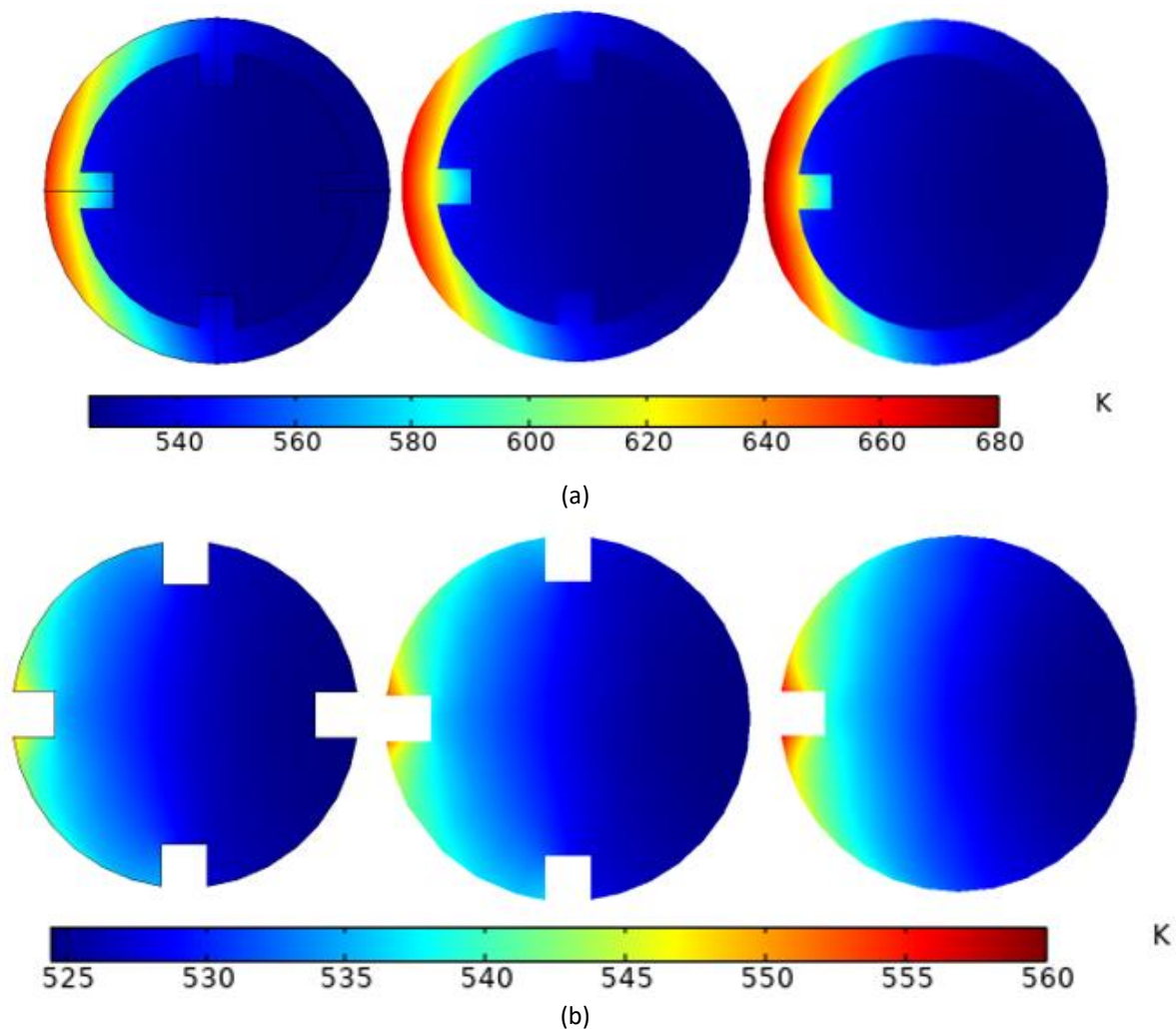


Fig. 8. Average Nusselt number with square internal fins ( $n=1, 3$  and  $4$ )

The temperature contour at the tube outlet for a square finned tube is displayed in Figure 9(a) below, the temperature variation in fluid area is not obviously displayed. Figure 9(b) shows the outlet

temperature contour in the fluid region only. As can be observed, the temperature distribution under non-uniform flux is inconsistent, with a hot region near the tube's heated half, where the maximum temperature in molten salt is 556 K in one square fin, which is larger than 4 square fins by 1.25%.



**Fig. 9.** Temperature contours with square internal fins ( $n=1, 3$  and  $4$ ) and  $Re=14,000$ : (a) for tube and fluid area, (b) for fluid area only

As illustrated in Figure 10, 11 and 12, even if the shape of the fins is changed to triangular, circular or rectangular with  $w=2$ , the same sequence as in the case of square fins persists. The Nusselt number is raised by an increase in the number of internal fins. The triangular finned tube registered the highest Nu, with the greatest boundary layer interruption. With  $n=4$  and  $Re=14000$ , the Nu was recorded as 111.13. And with  $Re=38000$  the Nu was recorded as 260.44. The rectangular-shaped fins consistently registered the lowest Nu.

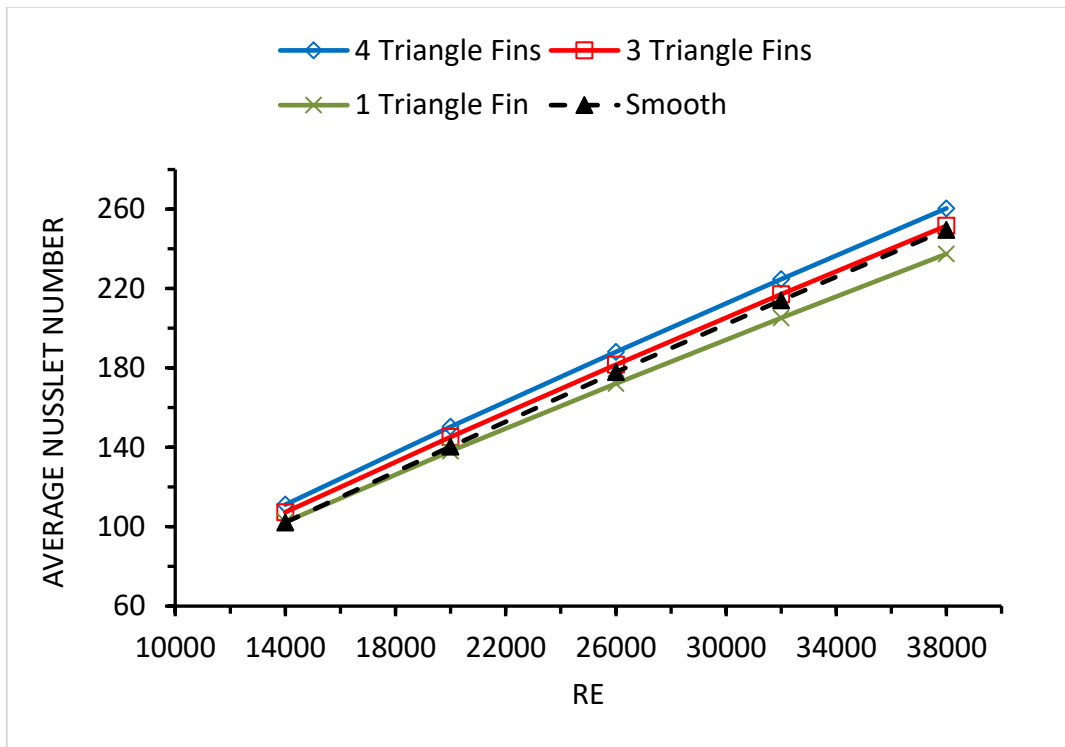


Fig. 10. Average Nusselt number with triangle internal fins (n=1, 3 and 4)

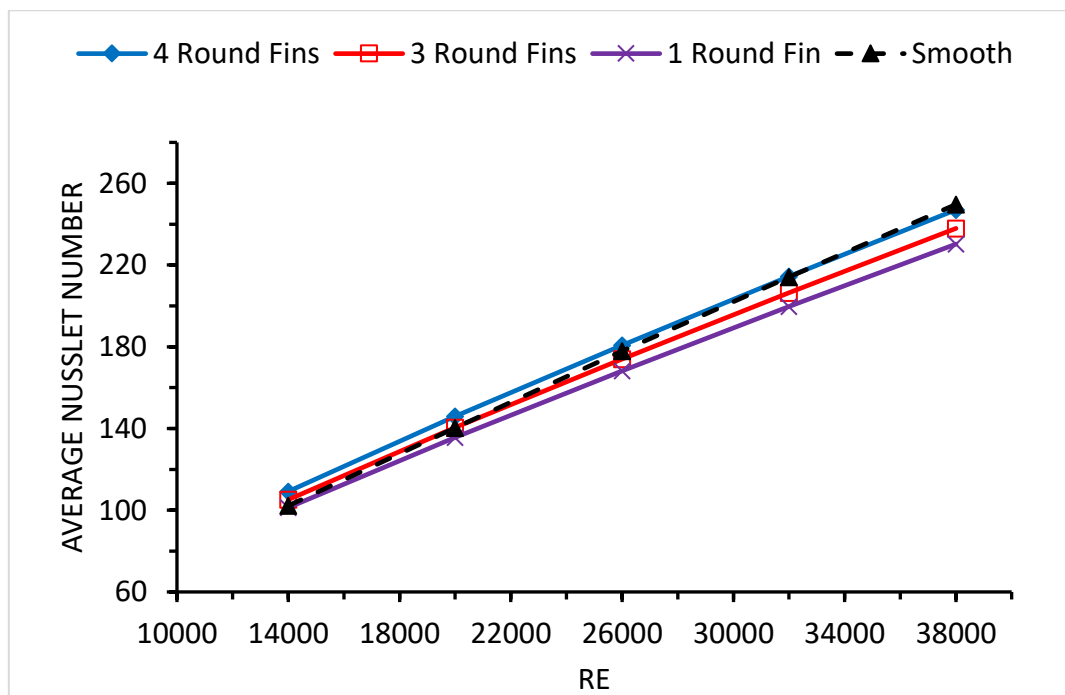
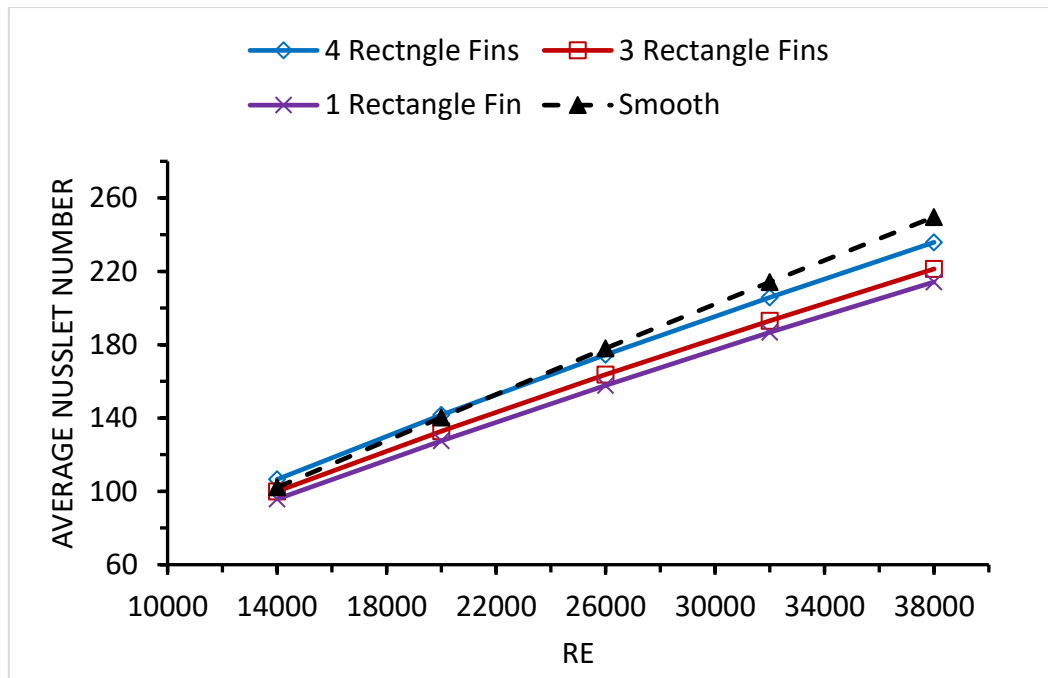
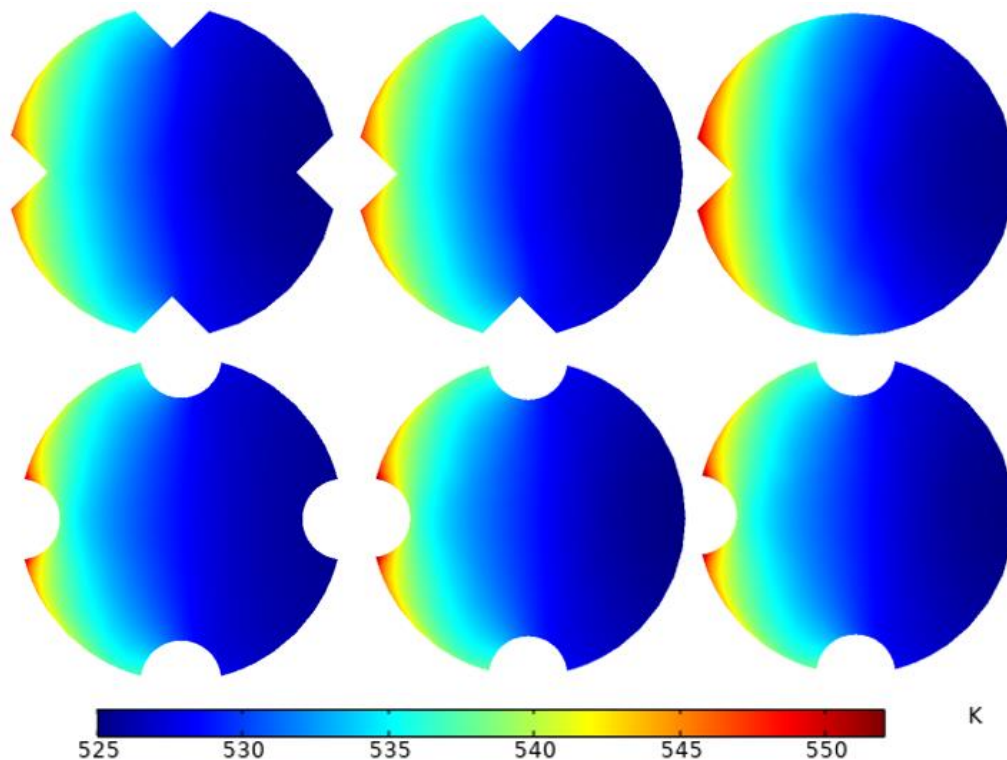


Fig. 11. Average Nusselt number with round internal fins (n=1, 3 and 4)



**Fig. 12.** Average Nusselt number with rectangle internal fins (n=1, 3 and 4)

Figure 13 illustrates the temperature contours based on the triangular and circular fins, where n has values of 1, 3 and 4 at the tube exit. It was observed that an increase in the fin number decreases the maximum temperature in molten salt area by the non-uniform heat flux. It was also observed that a lower value for the maximum temperature generates a larger Nu value, as well as lower values for thermal resistance and boundary layer thickness. This increased the molten salt temperature near the heated side.



**Fig. 13.** Temperature contours with regards to triangular and circular fins, where n=1, 3 and 4

#### 4.2 Effect of Differently Shaped Fins Under the Same Flow Rate

To study the effect of shape with the same flow rate, we considered the hydraulic area ( $A_h$ ) is the same. Following calculations, it became clear that the highest Nu is associated to the triangular fin. As displayed in Figure 14, with a flow rate of  $4.3 \text{ m}^3/\text{hour}$ , the triangular fin registered a Nu of 214.59. As the flow velocity in all the tubes is similar, the performance of the triangular fin, with an increment in Nu of 5% when  $Re=14000$ , and 7% when  $Re=38000$ , can be deemed superior.

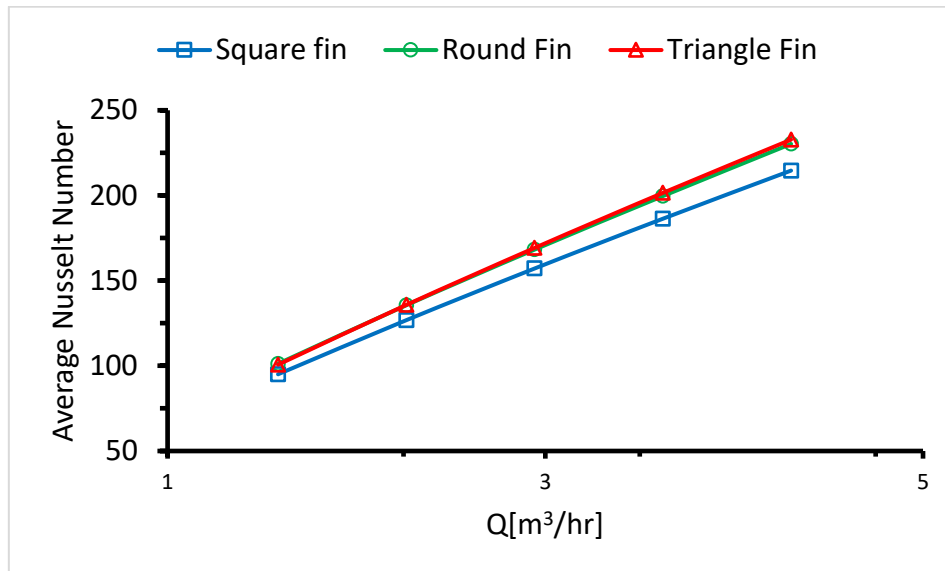


Fig. 14. Average Nusselt number with constant flow rate for  $n=1$

#### 4.3 Effect of Fin Shape

The influence of fin height for  $n=1$  with  $w = 1, 4, \text{ and } 6 \text{ mm}$ , is depicted in Figure 15. As can be observed, it is clear that the Nu increases with a reduction in the  $w$  values. The highest Nu is ascribed to triangular fins with  $w=1\text{mm}$ . The sharp edge of a triangular fin facilitates the separation of the boundary layers, and this increases the convection to enhance the Nu.

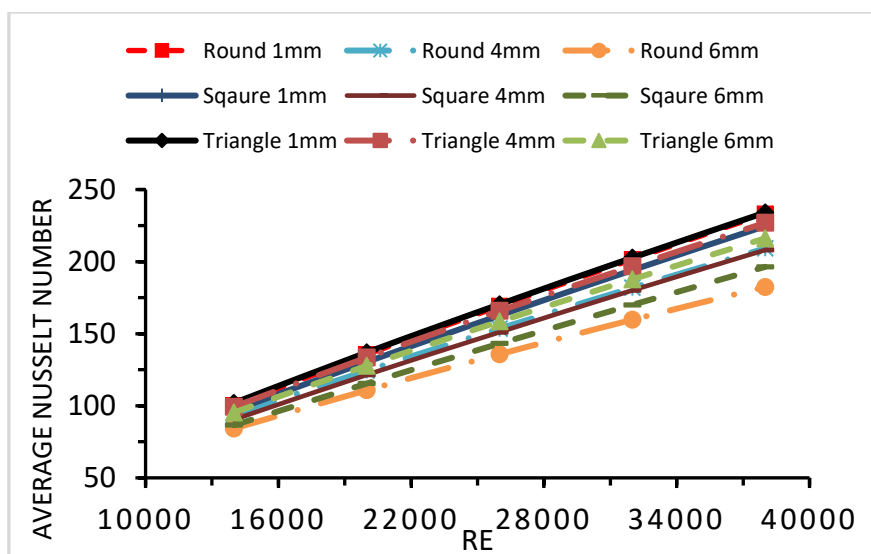
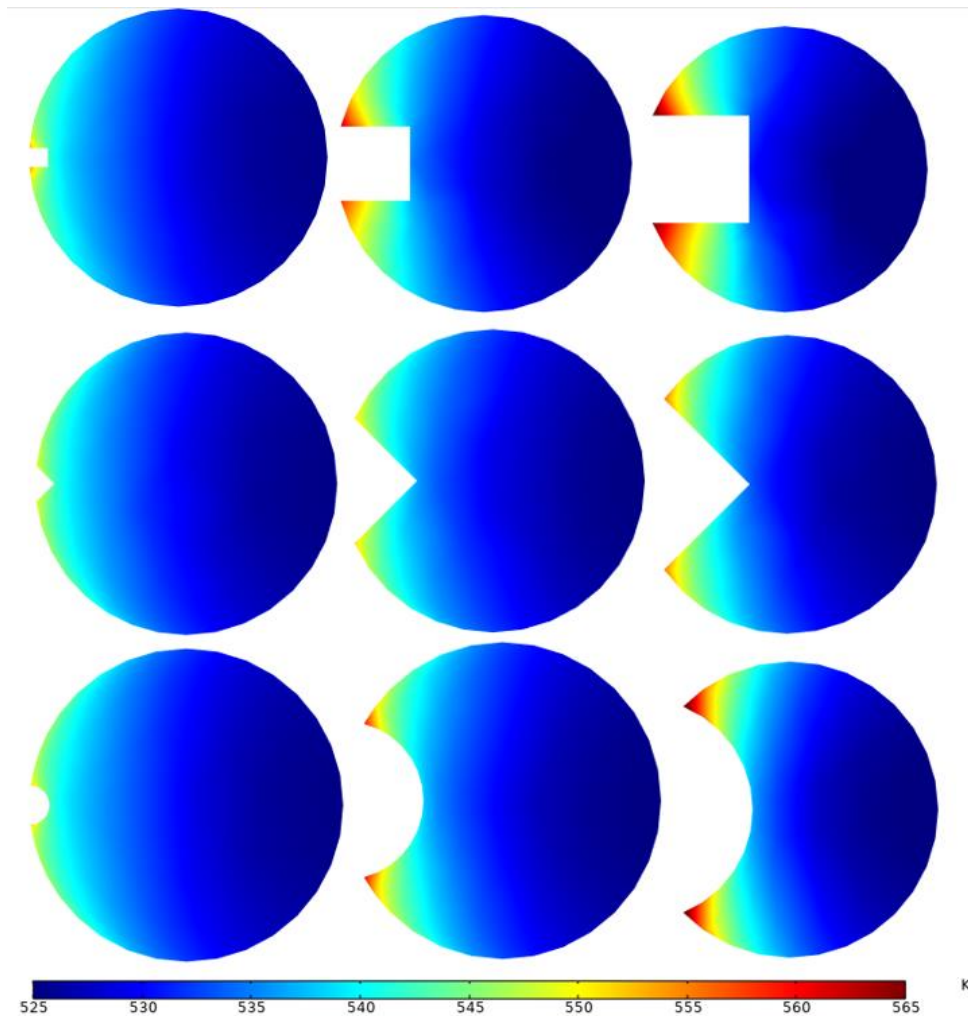
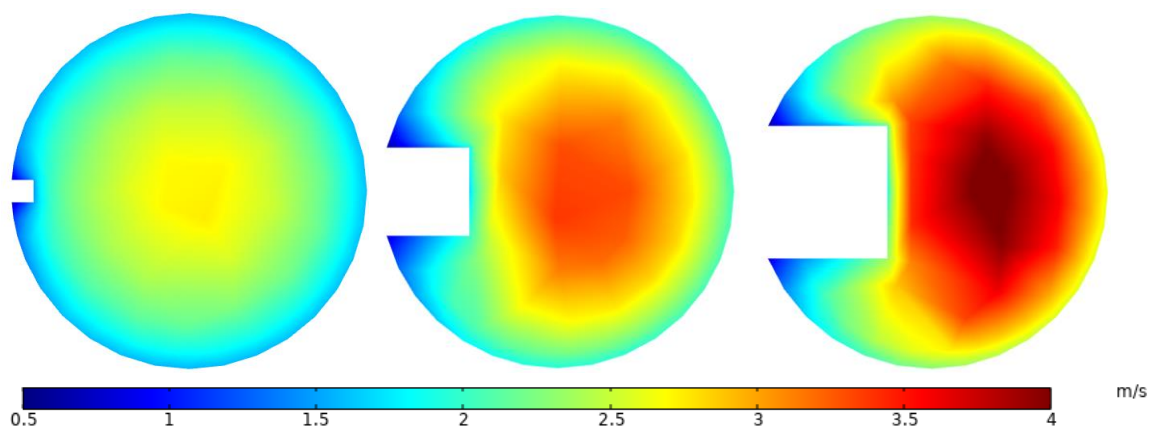


Fig. 15. Average Nusselt number with  $w=1, 4$  and  $6 \text{ mm}$  for square, triangular, and circular fins

Figure 16 shows the temperature contour, which depicts the rise in the maximum temperature of molten salt, with the increase in  $w$ . Increasing the fin height leads to wrapping of the flow area, and the thickening of the boundary layers, that raise the molten salt temperature close to the heated side. This is depicted in the velocity contours shown in Figure 17. An enhancement in the thickness of the boundary layers, serves to increase conduction, which ultimately leads to a reduction in  $Nu$ .



**Fig. 16.** Temperature contours with square, triangular and circular fins, where  $w=1, 4$  and  $6$  mm and  $Re=14,000$



**Fig. 17.** Velocity contours with square fins, where  $w=1, 4$  and  $6$  mm &  $Re=14,000$

### 4.4 Wall Temperature

Investigations were conducted on the effects of circumferential variations in the inner wall temperature, on the heated side, with different values of Reynolds numbers for a smooth tube, and for the square fin with  $n=1$ . As the pipe thickness increases, the stress ratio decay is reduced along the circumference. The temperature distribution in the pipe wall was decreased with the addition of internal fins, while the internal wetted area was increased. This is illustrated in Figure 18. It is clear that the addition of fins acutely reduced the wall temperature, near the outer maximum heat flux.

Figure 19 shows the heat transfer coefficient for a triangular fin with  $n=1$  and  $Re=14000$ , with a non-uniform heat flux. Unsurprisingly, the heat transfer coefficient was observed to be higher at the inlet of the tube, where the thermal boundary layer is thin. As the boundary layer increased, and the flow became more developed, the heat transfer coefficient decreased.

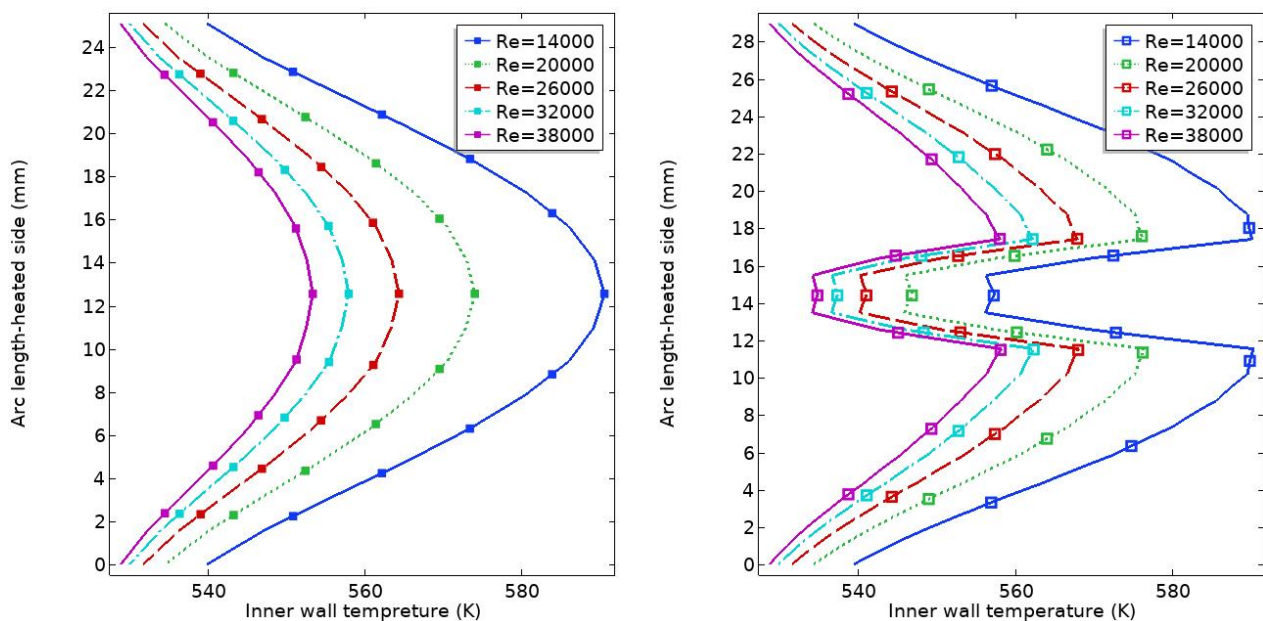


**Fig. 18.** Inner Wall temperature for smooth tube and for square fin with  $n=1$

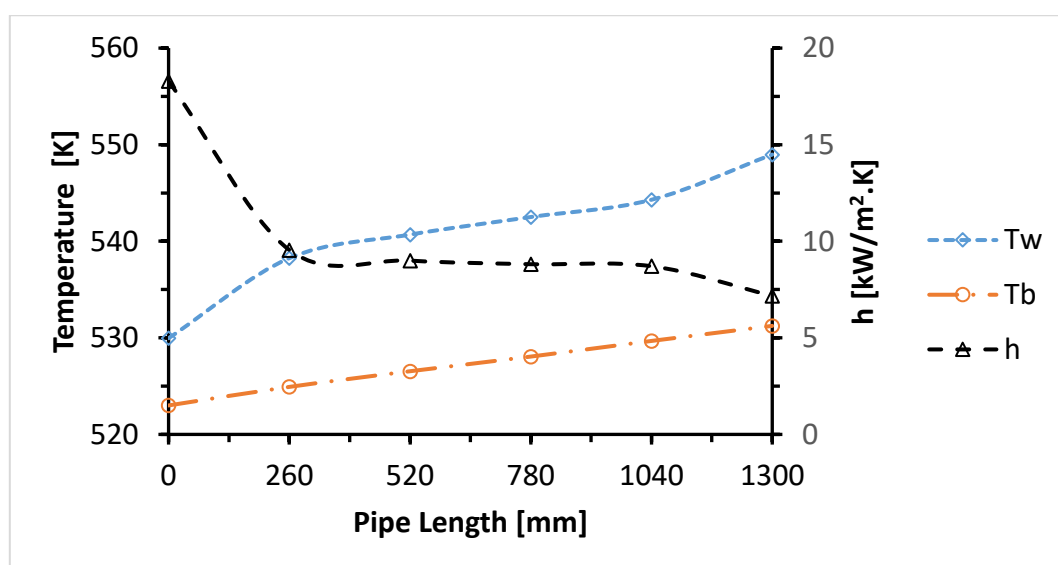


**Fig. 19.** Wall temperature, bulk temperature, and convective heat transfer coefficient for a triangular fin with  $Re=14000$

#### 4.5 Thermal Enhancement Factor (TEF)

Investigations on overall efficiency can be conducted through TEF, as depicted in Figure 20. A TEF higher than one is indicative of a turbulent flow rate. Effective thermal is higher for a low flow rate, as the heat transfer is enhanced by an increase in the residence time of the flow. The highest TEF was discerned near  $Re=14000$ . TEF decreases with the rise in  $Re$ . The highest TEF, which is consistently accompanied by  $n=4$ , stems from higher convection attributed to the interrupted development of the boundary layer, due to the decrease in hydraulic diameter, and the increase in flow velocity.

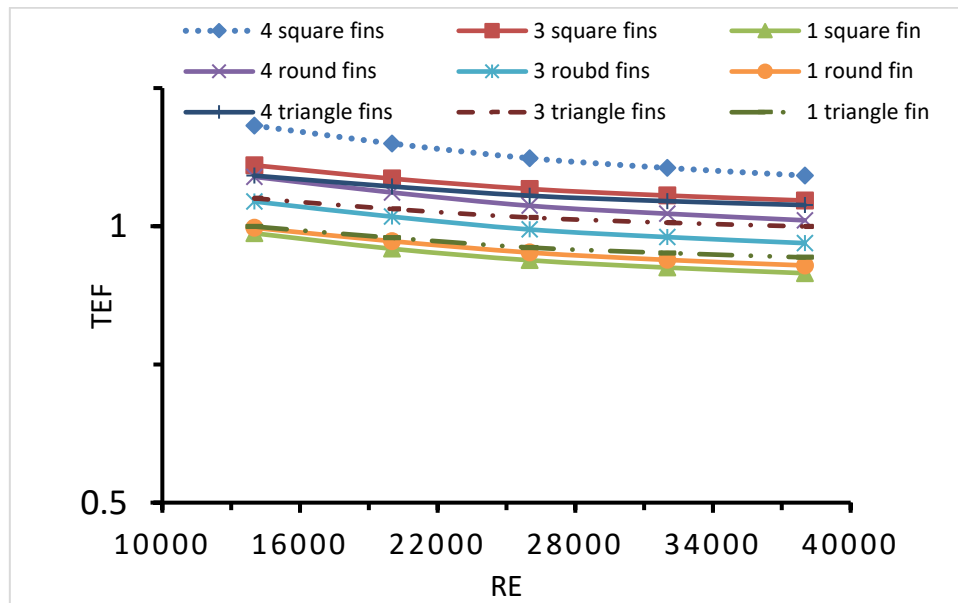


Fig. 20. TEF for square, triangular and circular fins with  $n=1, 3$  and  $4$

#### 4.6 Receiver Efficiency

The efficiency of the receiver increased slightly with an increase in Reynolds number. This is due to the fact that as seen in Figure 21, there is an increase in the convective coefficient with an increase in the mass flow rate. It was also observed that the triangular fins receiver exhibited maximum efficiency with lesser heat losses. Furthermore, as the internal area within the receiver rises (due to the addition of more fins); there is also an increase in heat losses as an effect of the receiver efficiency.

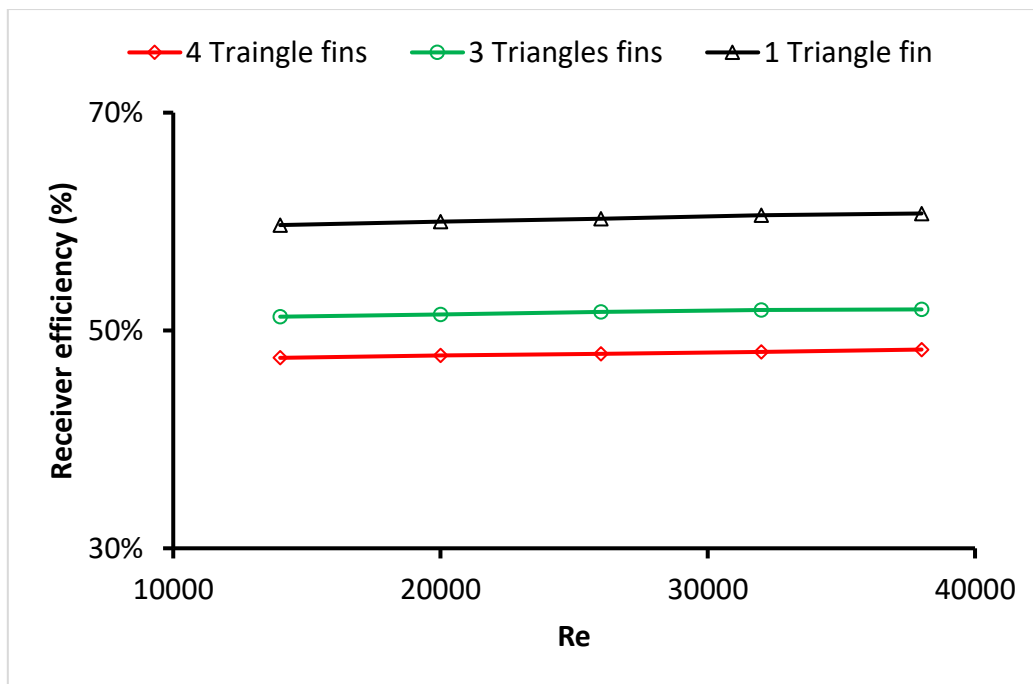


Fig. 21. Receiver collection efficiency with triangular fins (n=1,3, and 4)

## 5. Conclusions

With this undertaking, we propose a new molten salt solar receiver design. 3D simulation (through COMSOL multiphysics 5.5) involving differently shaped fins was performed to investigate the non-uniform hear flux effect on the external receiver. Molten salt was used as the heat transfer fluid. Variations in the Nusselt number, and the thermal enhancement factor versus the Reynolds number, for each case, were noted.

With  $n=4$  and square fins, a 12% increase in Nu was observed when the Re was at 14,000. However, this ratio declined with the increase in Re to arrive at 3.6% when the Re was at  $Re=38,000$ . While the addition of four triangular shaped fins raised the Nu to 8.7%, this ratio declined to 4.3% with the increase in Re. Thus, it can be surmised that close to Re 14,000, the best heat transfer enhancer is the square fin. On the other hand, when it comes to an elevated Re, the enhancement in heat transfer occurred with triangular shaped fins. When  $w=1$ , the best thermal enhancement factor was acquired through triangular shaped fins. For the same flow rate, and similar hydraulic area with one fin, the triangular fin proved to be the best heat transfer enhancer, with the greatest value close to a high Re.

In the context of a singular fin, the triangular fin proved to be superior, with the enhancement occurring only at  $Re=14000$ . The addition of internal fins, which reduces the inner wall temperature near the maximum heat flux by 6%, serves to extend the lifespan of the receiver. In the context of future work, we recommend more in-depth studies on the fins' thermal performance.

## References

- [1] Ma, Xinglong, Hongfei Zheng, and Shuli Liu. "A review on solar concentrators with multi-surface and multi-element combinations." *Journal of Daylighting* 6, no. 2 (2019): 80-96.  
<https://doi.org/10.15627/jd.2019.9>
- [2] Abu-Hamdeh, Nidal, and Khaled Alnefaie. "Techno-economic comparison of solar power tower system/photovoltaic system/wind turbine/diesel generator in supplying electrical energy to small loads." *Journal of Taibah University for Science* 13, no. 1 (2019): 216-224  
<https://doi.org/10.15627/jd.2019.9>

- [3] Nandakumar, K., and J. H. Masliyah. "Fully developed viscous flow in internally finned tubes." *The Chemical Engineering Journal* 10, no. 1 (1975): 113-120.  
[https://doi.org/10.1016/0300-9467\(75\)88025-7](https://doi.org/10.1016/0300-9467(75)88025-7)
- [4] Amina, Benabderrahmane, Aminallah Miloud, Laouedj Samir, Benazza Abdelylah, and J. P. Solano. "Heat transfer enhancement in a parabolic trough solar receiver using longitudinal fins and nanofluids." *Journal of thermal science* 25, no. 5 (2016): 410-417.  
<https://doi.org/10.1007/s11630-016-0878-3>
- [5] Piña-Ortiz, A., J. F. Hinojosa, R. A. Pérez-Enciso, V. M. Maytorena, R. A. Calleja, and C. A. Estrada. "Thermal analysis of a finned receiver for a central tower solar system." *Renewable Energy* 131 (2019): 1002-1012.  
<https://doi.org/10.1016/j.renene.2018.07.123>
- [6] Yang, Xiaoping, Xiaoxi Yang, Jing Ding, Youyuan Shao, and Hongbo Fan. "Numerical simulation study on the heat transfer characteristics of the tube receiver of the solar thermal power tower." *Applied Energy* 90, no. 1 (2012): 142-147.  
<https://doi.org/10.1016/j.apenergy.2011.07.006>
- [7] Hussein, A., M. S. Abd-Elhady, M. N. El-Sheikh, and H. T. El-Metwally. "Improving heat transfer through paraffin wax, by using fins and metallic strips." *Arabian Journal for Science and Engineering* 43, no. 9 (2018): 4433-4441.  
<https://doi.org/10.1007/s13369-017-2923-2>
- [8] Muñoz, Javier, and Alberto Abánades. "Analysis of internal helically finned tubes for parabolic trough design by CFD tools." *Applied energy* 88, no. 11 (2011): 4139-4149.  
<https://doi.org/10.1016/j.apenergy.2011.04.026>
- [9] Kumar, K. Ravi, and K. S. Reddy. "Thermal analysis of solar parabolic trough with porous disc receiver." *Applied Energy* 86, no. 9 (2009): 1804-1812.  
<https://doi.org/10.1016/j.apenergy.2008.11.007>
- [10] Gong, Xiangtao, Fuqiang Wang, Haiyan Wang, Jianyu Tan, Qingzhi Lai, and Huaizhi Han. "Heat transfer enhancement analysis of tube receiver for parabolic trough solar collector with pin fin arrays inserting." *Solar Energy* 144 (2017): 185-202.  
<https://doi.org/10.1016/j.solener.2017.01.020>
- [11] Rodríguez-Sánchez, M. R., A. Sánchez-González, C. Marugán-Cruz, and D. Santana. "New designs of molten-salt tubular-receiver for solar power tower." *Energy Procedia* 49 (2014): 504-513.
- [12] Zheng, Zhang-Jing, Ming-Jia Li, and Ya-Ling He. "Thermal analysis of solar central receiver tube with porous inserts and non-uniform heat flux." *Applied Energy* 185 (2017): 1152-1161.  
<https://doi.org/10.1016/j.apenergy.2015.11.039>
- [13] Changa, C., C. Xu, Z. Y. Wu, X. Li, Q. Q. Zhang, and Z. F. Wang. "Heat transfer enhancement and performance of solar thermal absorber tubes with circumferentially non-uniform heat flux." *Energy Procedia* 69, no. 1 (2015): 320-327.  
<https://doi.org/10.1016/j.egypro.2015.03.036>
- [14] Garbrecht, Oliver, Faruk Al-Sibai, Reinhold Kneer, and Kai Wieghardt. "CFD-simulation of a new receiver design for a molten salt solar power tower." *Solar Energy* 90 (2013): 94-106.  
<https://doi.org/10.1016/j.solener.2012.12.007>
- [15] Zhang, Yuwen, and A. Faghri. "Heat Transfer Enhancement in Latent Heat Thermal Energy Storage System by Using the Internally Finned Tube." *International Journal of Heat and Mass Transfer* 39, no. 15 (1996): 3165-73.  
[https://doi.org/10.1016/0017-9310\(95\)00402-5](https://doi.org/10.1016/0017-9310(95)00402-5)
- [16] Liu, Yun, Wen Jie Ye, Yong Hua Li, and Jin Fang Li. "Numerical Analysis of Inserts Configurations in a Cavity Receiver Tube of a Solar Power Tower Plant with Non-Uniform Heat Flux." *Applied Thermal Engineering* 140 (2018): 1-12.  
<https://doi.org/10.1016/j.applthermaleng.2018.05.016>
- [17] Baruah, Monoj, Anupam Dewan, and Pinakeswar Mahanta. "Performance of Elliptical Pin Fin Heat Exchanger with Three Elliptical Perforations." *CFD letters* 3, no. 2 (2011): 65-73.
- [18] Rout, Sachindra Kumar, Dipti Prasad Mishra, Dharendra Nath Thatoi, and Asit Ku Acharya. "Numerical Analysis of Mixed Convection through an Internally Finned Tube." *Advances in Mechanical Engineering* 2012 (2012).  
<https://doi.org/10.1155/2012/918342>
- [19] Albarbar, Alhussein, and Abdullah Arar. "Performance Assessment and Improvement of Central Receivers Used for Solar Thermal Plants." *Energies* 12, no. 16 (2019).  
<https://doi.org/10.3390/en12163079>
- [20] Neises, Ty W., Michael J. Wagner, and Allison K. Gray. *Structural design considerations for tubular power tower receivers operating at 650 C*. Vol. 45868. American Society of Mechanical Engineers, 2014.
- [21] Cengel, Y., and A. Ghajar. *Transient Heat Conduction*. Heat and Mass Transfer: Fundamentals and Applications; McGraw-Hill Education: New York, NY, USA, 2014.

- [22] Sánchez González, Alberto. "Heliostat field aiming strategies for solar central receivers." (2016).
- [23] Zavoico, Alexis B. *Solar power tower design basis document, Revision 0*. No. SAND2001-2100. Sandia National Labs., Albuquerque, NM (US); Sandia National Labs., Livermore, CA (US), 2001.
- [24] Dong, Xinyu, Qincheng Bi, and Fan Yao. "Experimental investigation on the heat transfer performance of molten salt flowing in an annular tube." *Experimental Thermal and Fluid Science* 102 (2019): 113-122.  
<https://doi.org/10.1016/j.expthermflusci.2018.11.003>
- [25] Debrah, Seth Kofi, Edward Shiitsi, Silas Chabi, and Neda Sahebi. "Assessment of heat transfer correlations in the sub-channels of proposed rod bundle geometry for supercritical water reactor." *Heliyon* 5, no. 11 (2019): e02927.  
<https://doi.org/10.1016/j.heliyon.2019.e02927>
- [26] Hajabdollahi, Hassan, Masoud Salarmofrad, Sajjad Shamsi, and Mohsen Rezaeian. "Numerical study of heat transfer and friction factor in a tube with groove and rib on the wall." *Heat Transfer* 49, no. 3 (2020): 1214-1236.  
<https://doi.org/10.1002/htj.21659>
- [27] Qiu, Yu, Ming-Jia Li, Meng-Jie Li, Hong-Hu Zhang, and Bo Ning. "Numerical and experimental study on heat transfer and flow features of representative molten salts for energy applications in turbulent tube flow." *International Journal of Heat and Mass Transfer* 135 (2019): 732-745.  
<https://doi.org/10.1016/j.egypro.2014.03.054>
- [28] Abdulwahab, Mohammed Raad. "A numerical investigation of turbulent magnetic nanofluid flow inside square straight channel." *Journal of Advanced Research in Fluid Mechanics and Thermal Sciences* 1, no. 1 (2014): 34-42.
- [29] Taler, Dawid, and Jan Taler. "Simple heat transfer correlations for turbulent tube flow." In *E3S Web of Conferences*, vol. 13, p. 02008. EDP Sciences, 2017.